Information Sciences 516 (2020) 56–71

Contents lists available at ScienceDirect

Information Sciences

journal homepage: www.elsevier.com/locate/ins

Pressure sensor placement in water distribution networks for leak detection using a hybrid information-entropy approach

Mohammad Sadegh Khorshidi[a], Mohammad Reza Nikoo[a,*], Narges Taravatrooy[a], Mojtaba Sadegh[b], Malik Al-Wardy[c], Ghazi Ali Al-Rawas[d]

[a] Department of Civil and Environmental Engineering, Shiraz University, Shiraz, Iran
[b] Department of Civil Engineering, Boise State University, USA
[c] Department of Soils, Water, and Agricultural Engineering, Sultan Qaboos University, Muscat, Oman
[d] Department of Civil and Architectural Engineering, Sultan Qaboos University, Muscat, Oman

ARTICLE INFO

Article history:
Received 23 September 2019
Revised 17 December 2019
Accepted 21 December 2019
Available online 24 December 2019

Keywords:
Pressure sensor placement
Leak detection
Transinformation entropy
Value of information
Water distribution network
ELECTRE model

ABSTRACT

This study proposes an optimization framework based on a hybrid information-entropy approach to identify leakage events in water distribution networks (WDN). Optimization-based methods are widely employed in the literature for such purposes; however, they are constrained by time-consuming procedures. Hence, researchers eliminate parts of the decision space to curtail the computational burden. Here, we propose an information theory-based approach, using Value of Information (VOI) and Transinformation Entropy (TE) methods, in conjunction with an optimization model to explore the entire decision space. VOI allows for the entire feasible space search through intelligent sampling, which in turn ensures robust solutions. TE minimizes redundant information and helps maximize the spatial distribution of sensors. The herein proposed model is developed within a multi-objective optimization framework that renders a set of Pareto-optimal solutions. ELimination and Choice Expressing the REality (ELECTRE) multi-criteria decision-making model is then used to select the best compromise solution given several weighting scenarios. The results of this study show that the information-entropy based scheme can improve the precision of leak detection by enhancing the decision space, and can reduce the computational burden.

1. Introduction

Increasing water demand and warming of the climate collectively reduced available water resources [5] and put an unprecedented toll on the water supply systems around the globe. Reduction of water loss in water distribution networks (WDNs) is, hence, of particular importance among water managers in this era of water shortage [32]. Leakage is the main cause of water loss in WDNs [10], which prompts pressure drop in the pipelines and in turn provokes consumer discontent. Leak detection is, therefore, of particular significance in any WDN. Accurate and well-timed leakage monitoring and detection prevent infrastructure failure, reduce lost revenue and avert excessive energy waste, and help maintain the provision of clean water to consumers.

* Corresponding author.
E-mail address: nikoo@shirazu.ac.ir (M.R. Nikoo).

https://doi.org/10.1016/j.ins.2019.12.043
0020-0255/

The exact identification of the quantity and location of leakage in WDNs requires costly detection instruments, such as Permalog acoustic devices [32]. While such highly accurate leak detection instruments are available in the market, the lower cost of installation and maintenance of pressure sensors and their acceptable measurement accuracy made them the most widely selected choice. Electronic pressure sensor devices usually use a silicon strain gauge whose resistance changes as pressure is applied to its surface. They use an integrated circuit to modify a reference signal based on the changes in the resistance of the strain gauge [6]. They are designed to measure pressure in different mediums such as liquids and gases, while providing high accuracy at a few decipascals level. The difference between pressure sensors' measurements and expected pressure values – obtained from simulation – can be attributed to leakage [31,32]. It is obviously ideal to install sensors at each joint of WDNs; however, the WDN sizes make deployment and maintenance of sensors at all joints unfeasible. Hence, computational frameworks are used to optimize the deployment of sensors in WDNs.

Researchers have developed various computational frameworks to detect leakage in WDNs and provide an optimum sensor deployment layout when only a limited number of sensors is feasible (e.g., [28,31]). Recent approaches use multi-objective optimization methods coupled with numerical models [31,32], which are focused on minimization of leak detection time and number of sensors [12,31,32]. Spatial coverage and mutual information are two important factors to consider when placing sensors, as they collectively play a key role in reducing time to leak detection and detection costs in WDNs. These aspects, however, were not fully explored in previous studies. Determining a set of representative pressure sensors that provide maximum information with minimum number of sensors is an effective strategy to reduce costs, as it warrants sufficient spatial coverage and maximum information [16,17,30]. The concept of Value of Information (VOI) is applied herein to identify a set of pressure sensor placements (nodes) that renders maximum information, as the first step for leak detection. The VOI concept has been applied in several areas of water science, including design of pollution warning systems in agricultural routine and WDNs [16,34], design of groundwater quality monitoring systems (e. g. [15]), flood monitoring (e. g. [1,2]), and reservoir water quality assessment [21]. However, to the best of the authors knowledge, VOI has not been explored for leak detection and pressure sensor placement in WDNs.

Different sensor layouts, even with a similar number of sensors and VOI, may yield different levels of redundancy (i.e. non-unique information). Hence, redundant information from monitoring stations should be minimized for optimal design to ensure maximum spatial coverage is provided by minimum number of sensors. Information redundancy of a given pair of sensors has a negative correlation with their spatial distance in a WDN. Therefore, minimizing information redundancy maximizes spatial distribution, and consequently, coverage of monitoring stations. Transinformation Entropy (TE) is one of the most potent methods to decrease mutual information between each pair of potential stations [30]. This method has been used in various branches of water science such as designing quality monitoring networks in reservoirs [29], rivers (e. g. [19,22]), and groundwater [20,23,24]; however, TE has not been used for leakage identification and placement of pressure sensors in a WDN.

Recently, a hybrid VOI-TE methodology has been proposed to maximize the reliability of sensor-provided information and minimize their redundancy in contamination warning systems for WDNs. This approach was also used to design monitoring networks of reservoir water quality [16,30]. The superior results of this methodology proved its efficacy and efficiency in the setting employed. However, the coupled VOI-TE approach has not been explored in the literature for leak detection in WDNs. In this study, an information-entropy based framework using VOI and TE approaches is developed to for optimal and effective sensor placement in WDNs. The literature has been mainly focused on optimization approaches, which – although being efficient – are associated with some weaknesses and shortcomings. Optimization approaches use multiple scenarios of simulated leakage events in an optimization framework to achieve the optimal layout of sensors for various objectives. However, due to the large size of simulations, exploring the entire decision spectra, i.e., all possible locations for installing pressure sensors, is associated with a prohibitive computational cost. Hence, eliminating parts of the decision space (i.e., all nodes proper for sensor placement) and determining pre-selected nodes as potential locations for placement of sensors is inevitable in these methods (e.g., [12,31,32]). This undermines the robustness of the obtained results.

Through the hybrid VOI-TE method proposed in this study, the simulation scenarios of leakage events are translated into a set of informatic curves. The optimum layout of sensors is accordingly determined by the set of curves with maximum union area AND minimum intersection area. Here, the term "optimum" refers to the objectives used as information metrics for defining the informatic curves. This approach significantly reduces the computational cost of the optimization framework and consequently allows for searching the entire decision spectra. The novelty of the proposed approach not only lies in the application of information theory in leak detection, but also in how it reduces the computational cost and improves the accuracy of leak detection of optimization-based methods. In this framework, the Non-dominated Sorting Genetic Algorithm II (NSGA-II) was used to maximize VOI and minimize TE, which collectively maximize coverage of sensors and minimize the number of pressure sensors. Efficacy of the proposed methodology was examined in the C-Town WDN.

2. Methodology

This study proposes a simulation-optimization framework based on the information and the entropy approaches using Value of Information (VOI) and Transinformation Entropy (TE). For the simulation part, a wide range of leakage scenarios that may occur in a Water Distribution Network (WDN) were simulated using the EPANET hydraulic model [35]. Then, using the simulations, numerical curves of VOI and TE are derived for each node. Next, the Non-dominated Sorting Genetic Algorithm-II (NSGA-II) multi-objective optimization model was developed considering three objectives: (1) minimizing

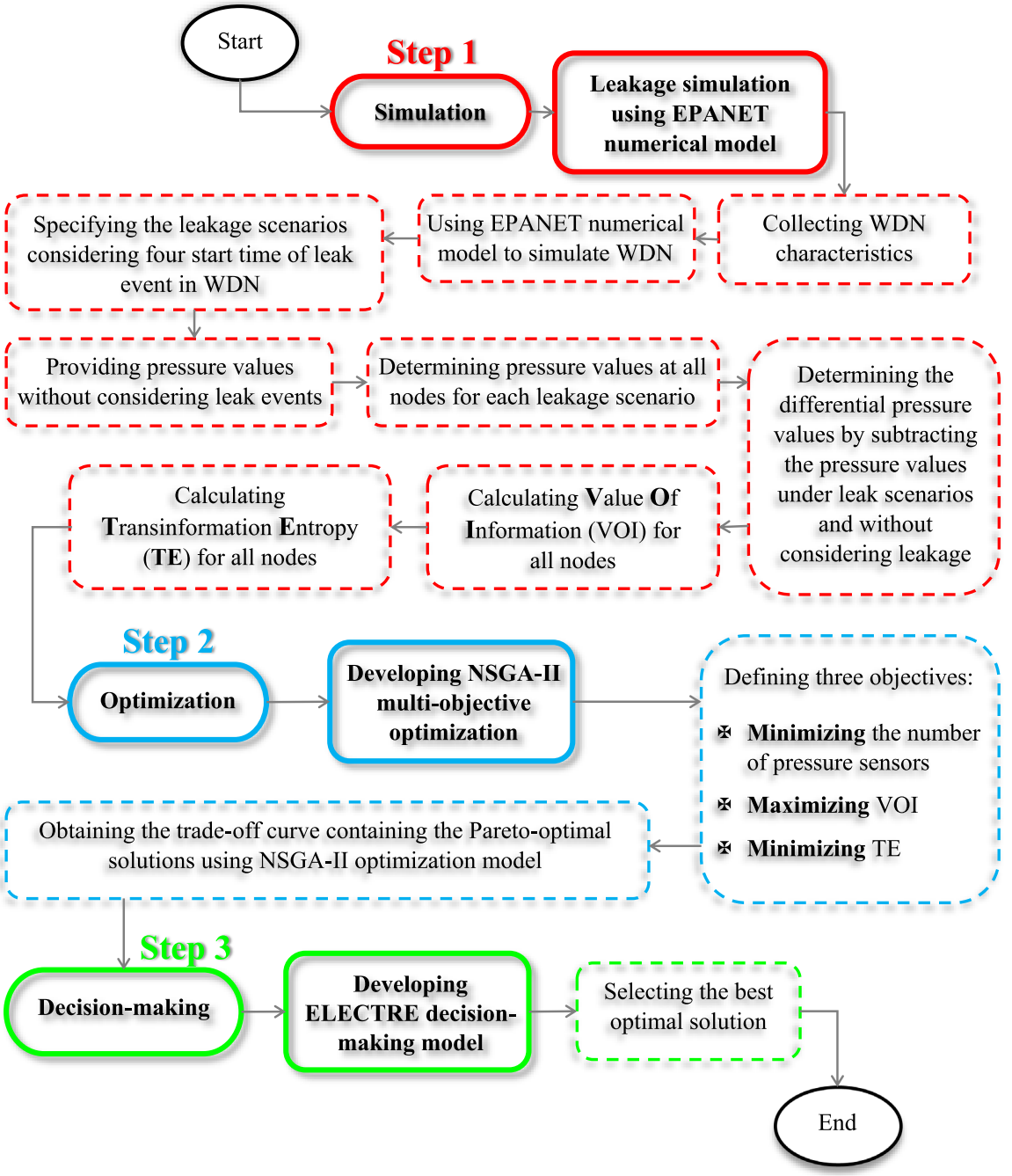

Fig. 1. Flow diagram of the proposed methodology of sensor placement in WDN for leak detection using a hybrid information-entropy approach.

number of sensors, (2) maximizing VOI, and (3) minimizing TE. Finally, to choose the optimal compromise solution between the NSGA-II results, the ELimination and Choice Expressing the REality (ELECTRE) decision-making model was applied [7,36]. These steps are illustrated in Fig. 1, and are discussed in detail in the following sections.

2.1. Leakage simulation in WDN

Leakage may occur in several forms, for example through circumferential cracks, longitudinal cracks, and round holes [39]. Herein, an orifice model (Eq. (1)) is employed to model leakage from a round hole with a flow equation defined as:

$$q = cp^{\gamma} \tag{1}$$

where,

q: leakage rate (liter per second);

p: pressure (Pa);

c: emitter coefficient (liter per second per $Pa^{0.5}$);

γ: pressure exponent; assumed to be 0.5 to model emitter as an orifice.

Since the EPANET model does not allow assigning emitter coefficients, and thereby cannot represent leakage, the leak scenarios were modeled as extra demand added to existing nodal demand based on the pressure values at each time step. The augmented demand of each node is represented as [32]:

$$Dnew_{n,i} = Din_{n,i} + \begin{cases} cp_{n,i}^{\gamma} & i \geq t_k \\ 0 & otherwise \end{cases} \quad \forall i \in 1,\ldots,T \text{ and } n \in 1,\ldots,N \tag{2}$$

where,

$Dnew_{n,i}$: new demand for node n at time-step i (in this study time-step is one hour);

$Din_{n,i}$: initial demand without leakage for node n at time-step i;

$p_{n,i}$: pressure at node n and time-step i;

γ: pressure exponent equal to 0.5;

c: emitter coefficient;

t_k: time-step at which leakage initiates at node n;

T: total number of simulation time-steps;

N: total number of nodes in WDN.

In this study, values of c (emitter coefficient) were tuned to generate leaks at a rate of 0.2–0.5 $\frac{lit}{sec}$. This range is selected to ensure a minimum change, set to pressure sensor's detectable threshold, occurs in the nodal pressure in the WDN. When leakage occurs, a different pressure profile is read from the nodes in the leakage zone than the expected pressure obtained from non-leakage scenario simulations. A similar behavior is observed when added demand is assigned to a node. Therefore, pressure sensors at the nodes within the leakage zone generate various pressure profiles depending on the start time and quantity of leakage.

Calculating an emitter coefficient (c) that generates a leak at the specified rate for any given node requires determining nodal pressure (p). Hence, the first step is to simulate the WDN using EPANET with no leakage (control state). The control state is simulated at a one-hour time step. The result is a $T \times N$ matrix, including nodal pressure values for a one-hour time step. For the leakage scenarios, we separate four time intervals around-the-clock (0-6, 6–12, 12–18, 18–24) to identify the influence of diurnal variation in nodal demand on the leakage amount.

It is ideal to simulate leakage at small increments, such as every 10 min, to thoroughly determine the influence of leakage in the network. However, this process is hugely time-consuming, and our preliminary sensitivity analysis shows that leakages create similar pressure reading patterns when variations in augmented demands are insignificant. In other words, the resulted nodal pressure patterns from leakages at a given node with close start times are rather similar. Therefore, only four time intervals during a day are considered as the start times of the leakage scenarios to reduce the simulation costs and avoid redundant analysis.

Subsequently, $4 \times N$ (i.e., four leakage time intervals times the number of nodes in a WDN) leakage scenarios are constructed using the augmented demand values calculated from Eq. (2), and simulated using EPANET. This yields $4 \times N$ matrices of size $T \times N$ containing nodal pressure values at each time-step for each leakage scenario. The matrices of nodal variation of pressure can be calculated by subtracting leakage pressure matrices from the control state pressure matrix.

Two vital parameters for performance assessment of leakage monitoring networks are: 1. Time elapsed between initiation of leakage and its detection by the monitoring network (hereafter, "time to detection"); and, 2. Quantity of leaked water (or wasted water). Both parameters should be minimized for all leakage scenario to obtain optimum sensor layout. To calculate these parameters, a tolerance pressure variation threshold should be defined. It is assumed that when the absolute difference between the pressure at node n and time-step i in any scenario and the corresponding nodal pressure in control state is greater than the defined threshold, leakage occurs in the WDN. To account for uncertainties associated with pressure reading and sensors' intrinsic measurement errors [32], we assumed a pressure threshold equal to 1 meter column of water in this study. Using the matrices of nodal pressure variation and the defined threshold, the time to detection of leakage at each node and the corresponding amount of leaked water in each scenario can be calculated. This results in two matrices of size $4N \times N$ whose elements in mth row and nth column are time to detection in the mth scenario and at the nth node and the corresponding amount of leaked water (or wasted water). These matrices are used to derive the values of VOI and TE.

2.2. Value of information (VOI)

One of the suitable approaches to desig leakage monitoring stations is the theory of Value of Information (VOI) [21]. Garyson [13] introduced this concept, and numerous researchers adopted the VOI approach for designing various monitoring networks [1,14]. According to the VOI theory, each potential sensor may have different states and messages with specific prior probability, $P(s)$. Each message influences the decision maker's opinion about the system's behavior. Whether or not the decision-maker's opinion is correct about the state of a system or a sensor, the received message may add value or cause

loss. Therefore, the opinion must be updated to achieve a more reliable decision at a specific node. The Bayes' theorem can be applied to assimilate the prior probability and the likelihood of an event:

$$P(s|m) = \frac{P(m|s)P(s)}{P(m)} \tag{3}$$

where,

$P(s|m)$: new opinion after receiving message m;

$P(m|s)$: conditional probability of receiving message m when the state of the system is s;

$P(s)$: prior probability of state s;

$P(m)$: probability of receiving message m.

State s for each node is defined as time to detection. Hence, vector $P(s)$ for all nodes can be determined using the time to detection matrix. Message m is interpreted as the leak event warning that the decision-maker receives via placing a sensor at a given node. The decision-maker places a sensor at node i to warn if leakage occurs at node j. When node j has the detection state s, the associated costs, $a(w, s)$, for a warning message, w, with several detection delay times can be defined. The effectiveness of warning messages in whether a message m is received, E_m, or not, E_n, can be calculated using Eqs. (4) and (5). Therefore, the value of a selected warning according to a received message m is determined by Eq. (6):

$$E_m = \sum_{ST} a(w, s)P(s|m) \tag{4}$$

$$E_n = \sum_{ST} a(w, s)P(s) \tag{5}$$

$$V_m = E_m - E_n \tag{6}$$

where, ST is the total number of detection states s. Eq. (7) calculates the VOI of node i to determine the state of node j ($VOI_i(j)$):

$$VOI_i(j) = \sum_{M_T} P(m)\left[\max_w\left(\sum_{S_T} a(w, s)P(s|m)\right) - \max_w\left(\sum_{S_T} a(w, s)P(s)\right)\right] \tag{7}$$

where, M_T is the total number of messages. Eq. (7) provides a numerical VOI curve through calculating $VOI_i(j)$ of a given node i for all other nodes. The VOI corresponding to node i for reading the entire system's state is equal to the area underneath the VOI_i curve. Noticeably, $VOI_i(i)$ always has the maximum value. If more than one node is chosen to detect the state of node j, the union of VOI curves of selected nodes is assumed as VOI curve of the set of nodes. For more details about VOI refer to Maymandi et al. [21].

2.3. Transinformation Entropy (TE)

Shannon [40] introduced the concept of entropy, which recently has gained wide applications in many fields of research (e. g. [3,8,9,33]). To obtain the mutual – i.e. overlapping – information in discrete form, also called "transinformation", between a pair of sensors placed at nodes i and j, Eq. (8) can be utilized. This equation calculates their Transinformation Entropy (TE) [23,24].

$$TE(i, j) = -\sum_{Si}\sum_{Sj} P(i_{si}, j_{sj}) \ln\left[\frac{P\left(i_{si}, j_{sj}\right)}{P(i_{si})P\left(j_{sj}\right)}\right] \tag{8}$$

where,

$P(i_{si}, j_{sj})$: joint probability of detecting state si at node i and sj at node j;

$P(i_{si})$: probability of detecting state si at node i;

$P(j_{sj})$: probability of detecting state sj at node j.

Similar to VOI, for more than one node, TE is the union of their TE curves. To warrant obtaining unique information from a set of nodes, TE should be minimized. For more details, refer to Singh [41] and Mogheir et al. [23,24].

Both VOI and TE could be calculated for any pair of nodes i and j in WDN. For this purpose, probabilities can be calculated using the derived time to detection and leaked water matrices from the simulated leakage scenarios. Note that the detection states and their related costs are arbitrary parameters that may differ depending on the decision-makers' priorities, and the size, shape and type of the WDN. The obtained values of VOI and TE can be stored in two matrices, where elements in the ith column and jth row correspond to $VOI_i(j)$ and $TE(i, j)$, respectively.

2.4. Multi-objective optimization

The NSGA-II multi-objective optimization model was developed in our proposed framework with three objectives: (1) minimizing number of pressure sensors, (2) maximizing VOI, and (3) minimizing TE. NSGA-II is powerful evolutionary algorithm that was introduced by Deb [11]. As a multi-objective algorithm, the NSGA-II performs elitism and crowding distance to choose the optimal solutions in the form of Pareto front [11] and ranks solutions based on dominance to find the non-dominated solutions [18,25,27,32].

The VOI and TE matrices that were calculated for all pairs of nodes are then used as inputs for the developed optimization model. A binary vector of decision variables ($\vec{d}$) is defined for the multi-objective optimization model. The size of this vector is equal to the number of nodes in WDN with values of 1 and 0 representing placing / not-pacing sensor at each node. Thus, the first objective (Z_1) of this optimization model, i.e. minimizing the the number of sensors, can be formulated as a summation of the elements of the decision vector (Eq. (9)). As mentioned earlier, the VOI of the exact set of nodes is the union of their VOI curves. In other words, the VOI of nodes i and j is equal to $\max\{VOI_i(l),\ VOI_j(l)\}, \forall l = 1, \ldots, n$; where l is a given node in the WDN. A set of nodes that provide maximum area underneath their union VOI curves would provide the maximum value to the decision-maker about the state of the WDN. The second objective function (Z_2) can be formulated as the summation of maximum of all selected rows of the VOI matrix calculated for all nodes (Eq. (10)). Similar to VOI, TE of a pair of nodes is the maximum of their specific TE. Hence, to minimize mutual information of the selected nodes (Z_3), one can minimize the summation of their TE union (Eq. (11)). Note that, in Eqs.10 and 11, all elements are divided by the maximum elements in VOI and TE matrices to normalize the results.

$$Minimize: Z_1 = \sum_{\forall i} d_i \tag{9}$$

$$Maximize: Z_2 = \frac{1}{\max\{VOI\}} \sum_{\forall j} \max_i \{d_i \times VOI_i(j)\} \tag{10}$$

$$Minimize: Z_3 = \frac{1}{\max\{TE\}} \sum_{\forall j \neq i} \max_i \left\{d_i \times d_j \times TE(i,j)\right\} \tag{11}$$

The number of decision variables in this model is equal to the number of nodes in WDN. To obtain a set of optimal locations for placement of sensors in WDNs, a population of decision vectors is defined. In the first generation, the NSGA-II model randomly generates a set of binary decision vectors, calculates their corresponding objective functions and their crowding distances. In the next generations, NSGA-II calculates a new set of decision vectors based on elitism, in an evolutionary manner, to improve the decision vectors' corresponding objective functions. This procedure continues to the point that NSGA-II is unable to find a decision vector with improved objectives compared to the existing ones in a relatively large number of generations. Given the multiobjective nature of the optimization procedure, the model finds the global optimal results and their corresponding objective functions as a Pareto-front curve/surface (depending on the number of objective functions). For further details about NSGA-II, refer to Deb [11].

2.5. ELECTRE decision-making model

Since all Pareto optimal solutions obtained from a multi-objective optimization model have the same level of worthiness, selecting the best compromise solution according to the decision-makers' priorities is challenging [25]. The ELimination and Choice Expressing the REality (ELECTRE) model, as a powerful decision-making tool, is one of the widely used choices in multi-criteria decision-making (MCDM) problems [7,36]. ELECTRE follows several steps to achieve the best compromise optimum solution among all those identified by NSGA-II [4]:

Assume that $A = \{a_1, \ldots, a_k\}$ is a vector of k possible alternatives and $C = \{c_1, \ldots, c_z\}$ is a vector of all z criteria. Matrix $M_{k\times z}$ can be formed as a decision matrix (Eq. (12)) in which the m_{ij} element represents the value of alternative ai according to criteria cj:

$$M_{k\times z} = \begin{array}{c} \\ a_1 \\ a_i \\ a_k \end{array} \begin{array}{c} \begin{array}{ccc} c_1 & c_j & c_z \end{array} \\ \begin{bmatrix} m_{11} & \cdots & m_{1z} \\ \vdots & m_{ij} & \vdots \\ m_{k1} & \cdots & m_{kz} \end{bmatrix} \end{array} \tag{12}$$

Subsequently, the normalized decision matrix ($N_{k\times z}$) will be constructed by normalizing values of m_{ij} using Eqs. (13) and (14):

$$n_{ij} = \frac{m_{ij}}{\sqrt{\sum_{i=1}^{k} m_{ij}^2}} \qquad i = 1, 2, \ldots, k \qquad j = 1, 2, \ldots, z \tag{13}$$

$$N_{k\times z}=\begin{bmatrix} n_{11} & \cdots & n_{1z} \\ \vdots & \ddots & \vdots \\ n_{k1} & \cdots & n_{kz} \end{bmatrix} \tag{14}$$

Then, considering several weighting scenarios, the weighted normalized decision matrix (U_{ij}) will be determined by multiplying the normalized matrix by the weights of each scenario:

$$U_{ij}^{r}=w_{j}^{r}\times N_{ij} \tag{15}$$

where, r is the weighting scenario's number.

In the next step, the concordance and discordance sets should be determined using Eqs. (16) and (17). Pairwise comparison is then made between the weighted normalized matrix elements, and the alternative with higher (superior) value is considered as the element of concordance set (Eq. (17)). The absolute difference between a pair of alternatives is considered as their discordance (Eq. (16)):

$$D_{gh}=\begin{cases} \left|U_{gj}-U_{hj}\right| & if\ g\neq h \\ 0 & if\ g=h \end{cases} \quad \forall\ j \tag{16}$$

$$C_{gh}=\begin{cases} 1 & if\ U_{gj}\geq U_{hj} \\ 0 & if\ U_{gj}<U_{hj} \end{cases} \quad \forall\ j \tag{17}$$

Subsequently, the concordance matrix is generated by multiplying the weights in each weighting scenario by the concordance elements. The summation of achieved values of each pair is the array of concordance matrix. Finally, the average of all elements in the matrix is determined. In the discordance set, the maximum value of all elements in each row is determined, and then their maximum value is set as the array of discordance matrix.

To form the net concordance matrix (NC) and the net discordance matrix (ND), i.e., binary matrices:

$$NC=\begin{cases} 1 & if\ C_{gh}\geq AvgC \\ 0 & if\ C_{gh}<AvgC \end{cases} \tag{18}$$

$$ND=\begin{cases} 1 & if\ D_{gh}<AvgD \\ 0 & if\ D_{gh}\geq AvgD \end{cases} \tag{19}$$

where, AvgC and AvgD are the average values of concordance and discordance matrices, respectively.

In the next step, the NC and ND matrices are multiplied, and the summation of each row and each column in the resulted matrx is determined. The difference between the value of rows and columns is set as the ELECTRE score. The alternative with the highest score is considered the best solution.

3. Case study

The proposed methodology was examined on the WDN of the C-Town as a virtual city, which is a widely used case study in the literature. The data of real-world WDNs are usually not available for research due to security reasons. The proposed methodology is, however, general and can be applied to real-world case studies, if their WDN setting is available. C-Town is designed as a very complex network, and real-world WDNs of the same size are usually less complex. Given the methodological nature of this study, the C-Town WDN serves as a perfect case study. This WDN comprises of 388 nodes in five elevation categories, one reservoir, 11 pumps, and seven water tanks (Fig. 2). As discussed earlier, four leakage start times are defined, including 12 am, 6 am, 12 pm, and 6 pm for leakage from all nodes in the WDN.

Considering 388 nodes of the C-Town WDN and four leakage start times, we have 1552 (388×4=1552) leakage scenarios. The EPANET numerical hydraulic model [35] is employed to simulate the WDN for the mentioned leakage scenarios for the duration of 96 h. For each scenario, a nodal pressure variation matrix is calculated, as discussed in Section 2.1.

4. Results

As mentioned earlier, time to detection of leak events at each node was considered as a detection state. Seven detection states are defined (Fig. 3) to calculate the VOI for each node. In case of leakage in the WDN, fast detection of leak events would prevent damages to infrastructure and pollution backwash into the pipeline. Detection of leakage in the first interval (between 0 to 1 h) is associated with the least destructive consequences. On the contrary, detecting leakage in stage 7, i.e., between 60 and 96 h after the occurrence of leakage, would cause the highest damage. As shown in Fig. 3, the intervals are not equidistant, because lower delays in detection of leakage are of the highest priority. For example, it is important to detect leakage in the first 30 min as compared to the first two hours. On the other hand, relative differences in losses of detecting leakage in 70 h and 90 h from leakage are small.

The cost matrix, $a(w, s)$, is required to calculate VOI. This matrix indicates the associated costs of determining the detection state of node j via a sensor placed at node i. In other words, detecting leakage at time w following the receipt of

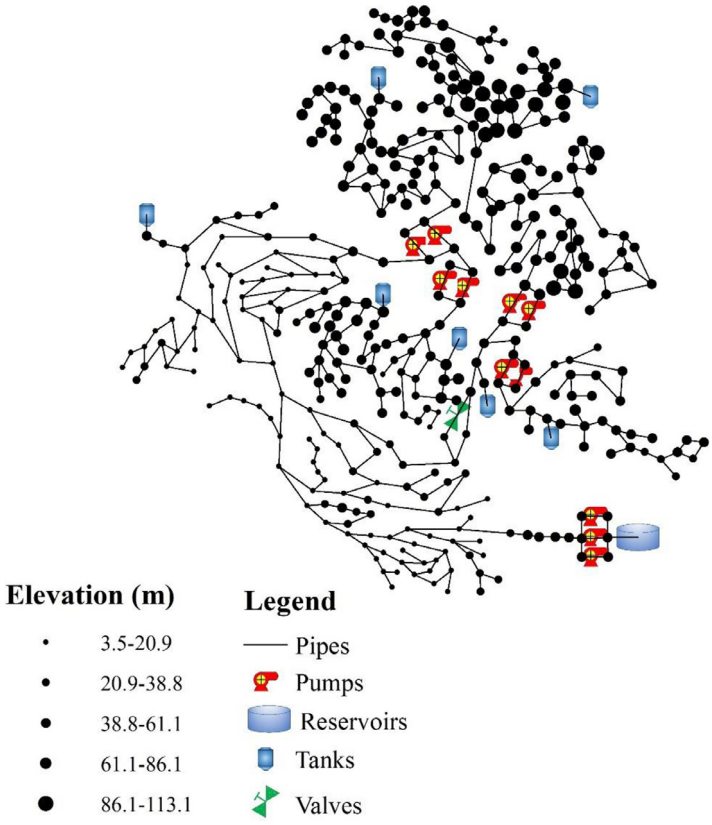

Fig. 2. C-Town water distribution network and its characteristics.

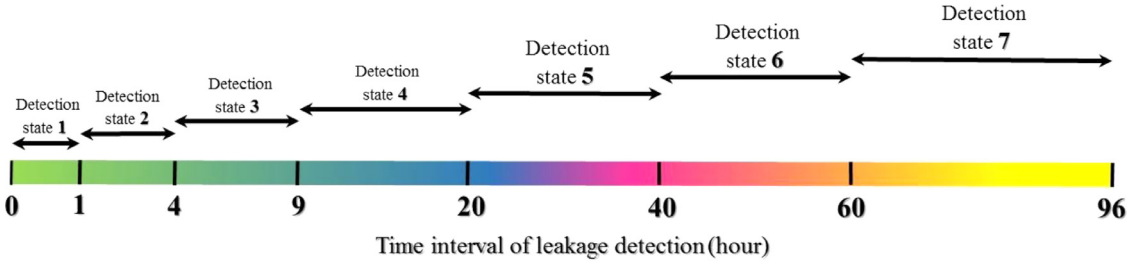

Fig. 3. Detection states, *s*, as defined by the time interval between the occurrence of leakage and its detection by a pressure sensor at a given node.

Table 1
Maximum volume of leaked water in the simulated scenarios in each defined detection state, *s*.

	s_1	s_2	s_3	s_4	s_5	s_6	s_7
Loss (liters)	432	2160	3456	6652	28116	98842	172800

message *m*, i.e., leakage warning, from a sensor placed at node *i*, when the leakage was actually detectable in time *s* at node *j* (the detection state of node *j* was *s*) would cost $a(w, s)$. As discussed in Section 2.3, both detection state, *s*, and cost matrix, $a(w, s)$, are arbitrary parameters that are defined based on the decision-makers' opinions and priorities and may vary on a case by case basis. Here, we considered the amount of leaked water as the costs associated with delays in detecting leakage in WDN. For this, we used the leaked water matrix calculated in Section 2.1 for all leakage scenarios to determine the maximum volume of leaked water for various delay levels in detecting leakage. Table 1 shows the calculated maximum loss, i.e., the volume of leaked water when the detection state at a given node is *s*.

The cost matrix, $a(w, s)$, can be calculated assuming that time delays, *w*, can be defined in the same way that detection state, *s*, was defined. Hence, there would be seven delay levels (i.e., $w_1, \ldots, w_7$). Each $a(w_i, s_j)$ can be calculated as the

Table 2
Cost associated with different warning lags in each detection state for the VOI calculation.

	Cost, $a(w, s)$ of detecting leakage at time, w, when the detection state of WDN was s						
	w_1	w_2	w_3	w_4	w_5	w_6	w_7
S_1	0	-1728	-3024	-6220	-27734	-98410	-172368
S_2	-1728	0	-1296	-4492	-26006	-96682	-170640
S_3	-3024	-1296	0	-3196	-24710	-95386	-169344
S_4	-6220	-4492	-3196	0	-21514	-92189	-166147
S_5	-27734	-26006	-24710	-21514	0	-70675	-144633
S_6	-98410	-96682	-95386	-92189	-70675	0	-73958
S_7	-172368	-170640	-169344	-166147	-144633	-73958	0

Table 3
Leak detection probabilities for nodes 5 and 118 in seven detection states.

Detection state	$P(s)$	
	Node No. 5	Node No. 118
s_1	0.00	0.00
s_2	0.00	0.00
s_3	0.06	0.15
s_4	0.13	0.44
s_5	0.11	0.00
s_6	0.11	0.03
s_7	0.57	0.37

difference between the amount of leaked water given sensor at node i detects leakage with a time delay w_i, versus it would have been detected by a sensor at node j at time s_j. Applying this procedure for all time delays and all detection states would result in cost matrix, $a(w, s)$, as provided in Table 2. Since $a(w, s)$ is of cost nature, a negative sign is assigned to the obtained values to accommodate minimization of objectives. When there is no time delay in predicting the detection state of node j, i.e., sensor is also placed at node j, the associated cost is 0. Thus, the diagonal elements of $a(w, s)$ are 0.

Another parameter that is required for calculation of VOI is the vectors of prior and posterior probabilities for each node. From the 1552 simulated leakage scenarios, 80% and 20% are used to derive the vectors of prior and posterior probabilities for each node, respectively. As an example, Table 3 presents the values of $P(s)$ for different detection states for nodes 5 and 118. The probability of detecting leakage under 20 h (detection state #4) when sensor is placed at node 5 is about 19% (0+0+6+13=19) while placing a pressure sensor at node 118 provides 59% (0+0+15+44=59) probability of detecting leakage under the mentioned time. Also, if sensors are placed at both nodes 5 and 118, there would be no detection in the first 4 h from the leakage occurrence.

Subsequently, for all pairs of nodes, VOI and TE are determined using the procedure discussed in Sections 2.2 and 2.3. The results are two square matrices with a size of 388×388, which contain values of $VOI_i(j)$ and $TE(i, j)$ in their ith row and jth column assuming a sensor is placed at node i to determine the detection state at node j. Thus, the ith row of the VOI matrix shows the value of information that a sensor placed at node i could provide to determine the detection state in other nodes, while the same row in the TE matrix shows the mutual information that a sensor at node i would have had if other sensors were also placed at other nodes. For more clarity, values in the VOI and TE matrices are normalized against their greatest element.

A value of 1 in the ith row and jth column of the VOI matrix indicates that regardless of whether the sensor is placed at node i or node j, it will provide the same value to the decision-makers. On the other hand, a value of 0 would indicate that placing a sensor at node i would not provide any information about the detection state of node j. The same element in the TE matrix would indicate complete information redundancy, if it is equal to 1, and complete information uniqueness if equal to 0. To provide a graphical example of this interpretation, the values of normalized VOI assuming sensors are placed at nodes 5 and 118 for determining detection state of all other nodes are provided in Fig. 4a and 4c. The information redundancy of a sensor placed at these nodes against all other nodes is displayed in Fig. 4b and 4d. This figure clearly demonstrates the dependency of TE and VOI on the spatial distance between sensors [16], and serves an example on how this data can be visualized for all nodes.

In the next step, the NSGA-II multi-objective optimization model is executed to find the set of sensor layouts with the minimum number of sensors, maximum VOI, and minimum TE. The examination of initial results obtained from the optimization model shows that the model retrieved a set of Pareto optimal layouts composed of 30 to 90 sensors. Since the main purpose of implementing this methodology is to minimize the total cost of leak detection in WDN, the number of pressure sensors plays a vital role [32]. Thus, we constrained the model to select sensor layouts with less than 10 sensors. Since our proposed approach significantly reduced the computational cost of the optimization framework, we can define a relatively large population size of 200 for NSGA-II. The maximum number of generations in NSGA-II is set to 2000 gener-

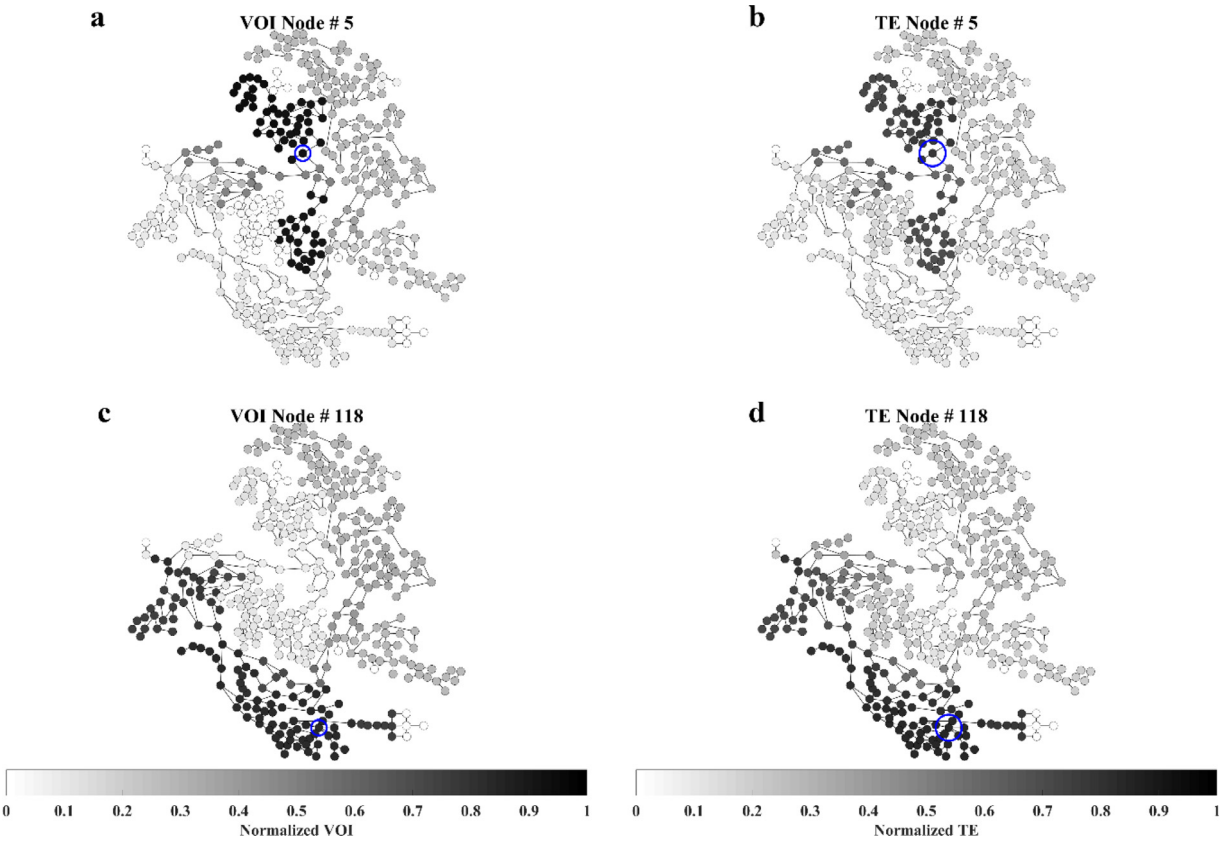

Fig. 4. Normalized VOI for nodes 5 (a), and 118 (c), and normalized TE for nodes 5 (b) and 118 (d) of the C-Town WDN.

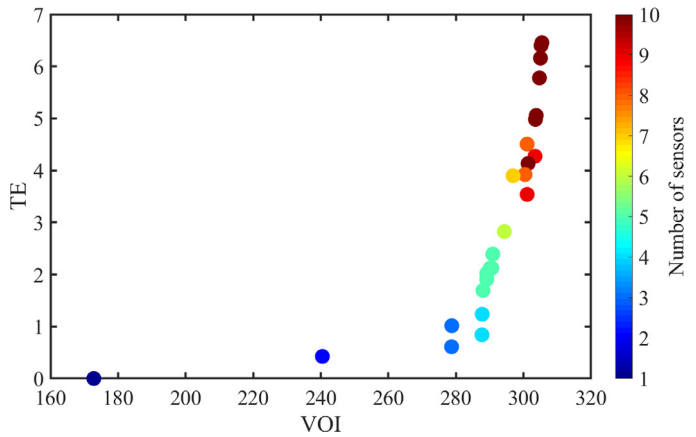

Fig. 5. Trade-off curve between three objectives defined in the NSGA-II multi-objective optimization model; i.e., minimization of the number of sensors (shown by the color bar); maximization of VOI (horizontal axis) and minimization of TE (vertical axis).

ations to ensure that the optimization model reaches convergence. The stopping criteria of the model, "StallGenLimit", is defined based on the convergence of the model to ensure obtaining globally optimal solutions. This criterion implies that if the model was not able to further improve the results after a certain number of generations, it would stop and retrieve the obtained decision vectors and their corresponding objective functions as globally optimal solutions and Pareto-front, respectively. StallGenLimit is set to 50 generations. The resulted optimal solutions by the NSGA-II model are presented in Fig. 5. Thirty optimal layouts are rendered in this step.

VOI and TE are used as metrics to find the optimal layout of sensors. However, vital parameters that are used for performance assessment of any designed layout are their capability of detecting leakage; i.e., probability of detecting leakage in WDN through deploying the designed sensors (*Pd*); average time between occurrence of probable leakage and its detection

Table 4
Pareto-optimal layout of pressure sensors, their corresponding objective function values, probabilities of detecting a leakage scenario, *Pd*, average time to detection, *Td*, and average quantity of leaked water in the simulated scenarios, *Wd*.

# Pareto point	Number of sensors	Node labels for placement of sensors	VOI	TE	*Pd*	*Td* (min)	*Wd* (m^3)
1	10	{11,33,85,107,129,147,171,235,319,375}	305.44	6.46	0.99	1217	94.67
2	10	{11,33,85,106,129,147,171,235,319,374}	305.2	6.4	0.99	1217	94.67
3	10	{71,107,111,129,130,160,291,349,366,384}	305.02	6.16	0.99	1237	96.14
4	10	{214,227,259,299,303,323,353,366,381,386}	304.72	5.78	0.99	1237	96.14
5	10	{8,17,21,24,59,79,109,245,342,383}	303.76	5.06	0.99	1206	93.85
6	10	{8,18,22,24,59,79,109,246,342,383}	303.54	4.98	0.99	1206	93.85
7	10	{8,18,21,24,59,79,109,246,342,383}	303.54	4.98	0.99	1206	93.85
8	9	{147,217,287,291,293,322,331,346,353}	303.41	4.27	0.99	1237	96.14
9	10	{147,217,287,292,293,322,331,332,345,353}	301.36	4.13	0.99	1237	96.14
10	9	{148,217,287,292,293,322,332,345,353}	301.08	3.54	0.99	1237	96.14
11	8	{67,87,126,140,142,167,212,289}	301.07	4.51	0.99	1237	96.13
12	8	{148,217,287,293,321,332,345,353}	300.44	3.92	0.99	1237	96.14
13	7	{189,342,350,351,357,358,387}	296.92	3.9	0.99	1280	99.38
14	6	{341,352,373,383,384,388}	294.33	2.82	0.99	1242	96.54
15	5	{360,364,378,387,388}	290.91	2.39	0.99	1337	103.67
16	5	{365,380,384,387,388}	290.62	2.12	0.99	1311	101.71
17	5	{365,380,385,387,388}	290.12	2.12	0.99	1311	101.71
18	5	{365,380,386,387,388}	289.11	2.02	0.99	1326	102.85
19	5	{365,380,382,387,388}	289.1	1.91	0.99	1237	96.14
20	5	{365,380,381,387,388}	288	1.69	0.99	1311	101.71
21	4	{360,378,387,388}	287.77	1.24	0.99	1337	103.67
22	4	{365,379,387,388}	287.71	0.84	0.99	1337	103.67
23	3	{360,387,388}	278.77	1.02	0.99	1337	103.67
24	3	{365,387,388}	278.71	0.61	0.99	1337	103.67
25	2	{387,388}	240.47	0.42	0.98	2720	208.12
26	2	{387,388}	240.47	0.42	0.98	2720	208.12
27	2	{387,388}	240.47	0.42	0.98	2720	208.12
28	2	{387,388}	240.47	0.42	0.98	2720	208.12
29	2	{387,388}	240.47	0.42	0.98	2720	208.12
30	1	{388}	172.81	0	0.48	2062	300.36
R1	10	{27,33,37,63,119,163,246,342,349,358}	301.28	6.14	0.99	1221	94.95
R2	10	{58,70,116,134,236,274,284,297,342,355}	273.94	8.11	0.99	1578	121.75
R3	10	{38,86,90,276,284,336,343,349,358,384}	240.15	7.29	0.99	1311	101.7

by the designed layout (*Td*), and average quantity of wasted water before detecting the leakage event in WDN (*Wd*). These parameters can be calculated using the 1552 simulated leakage scenarios. For a given layout of sensors from the 30 obtained layouts, the probability of detecting leakage, *Pd*, can be calculated as the number of scenarios in which the layout of sensors is capable of detecting leakage divided by the total number of leakage scenarios. Average time to detection, *Td*, is the average of time intervals between the occurrence of leakage in each scenario and its detection by the designed layout. For the quantity of leaked water, *Wd*, the volume of leakage before the detection of leakage event in each scenario can easily be calculated for any designed layout of sensors via the leaked water matrix derived from simulations described in Section 2.1.

Table 4 presents Pareto-optimal solutions in terms of the three objectives of this study, and their corresponding values of probability of detecting a leakage event (*Pd*), average time to detection (*Td*), and average leaked volume of water (*Wd*). Also, the values of these parameters are calculated for the three sets of sensors reported in Raei et al. [32] to compare the performance of our proposed framework against theirs. These three sets of sensors are denoted by R1, R2, and R3 in Table 4. In the case of only one pressure sensor (Pareto point # 30), about half of leakage scenarios are detectable, while five or more sensors would result in detecting leakage in more than 98% of leakage scenarios.

We may now compare the obtained Pareto optimal layouts with 10 sensors with the layouts (with a similar number of sensors) reported in Raei et al. [32]. Interestingly, the values of VOI for R1, R2, and R3 are smaller than those of Pareto point # 1,2,3,4,5,6,7, and 9, which indicates the lower information value that these sensor layouts provide to the decision-maker compared to the layouts of the herein derived Pareto points. On the contrary, the values of TE for R2 and R3 are greater than those of the Pareto points, while the value of TE for R1 is roughly equal to that of Pareto points #1, 2, and 3. This shows that deploying R1, R2, and R3 would provide more redundant information to the decision-maker compared to the layouts of the Pareto points. Comparing the provided metrics for performance assessment of the designed layouts, i.e., Pareto point, with those of R1, R2, and R3, further attests to the robustness and superiority of the herein proposed framework compared to the previous methods. While the probabilities of detecting leakage scenarios, *Pd*, provided by R1, R2, and R3 layouts are similar to those provided by the layouts of Pareto points, other parameters, i.e., average time to detection, *Td*, and average volume of leaked water, *Wd*, are widely different. *Td* for the Pareto layouts are in the range of 1206 min to 1237 min, while only R1 lies in this range with a *Td* of 1221 min. *Td* for R2 and R3 are out of this range with average time to detection of 1578 and 1311 min, respectively. Same can be stated for the volume of leaked water, as *Wd* for the Pareto point layouts with 10 sensors is in the range of 93.85 m^3 to 96.14 m^3, and only the average volume of leaked water for R1 falls in this

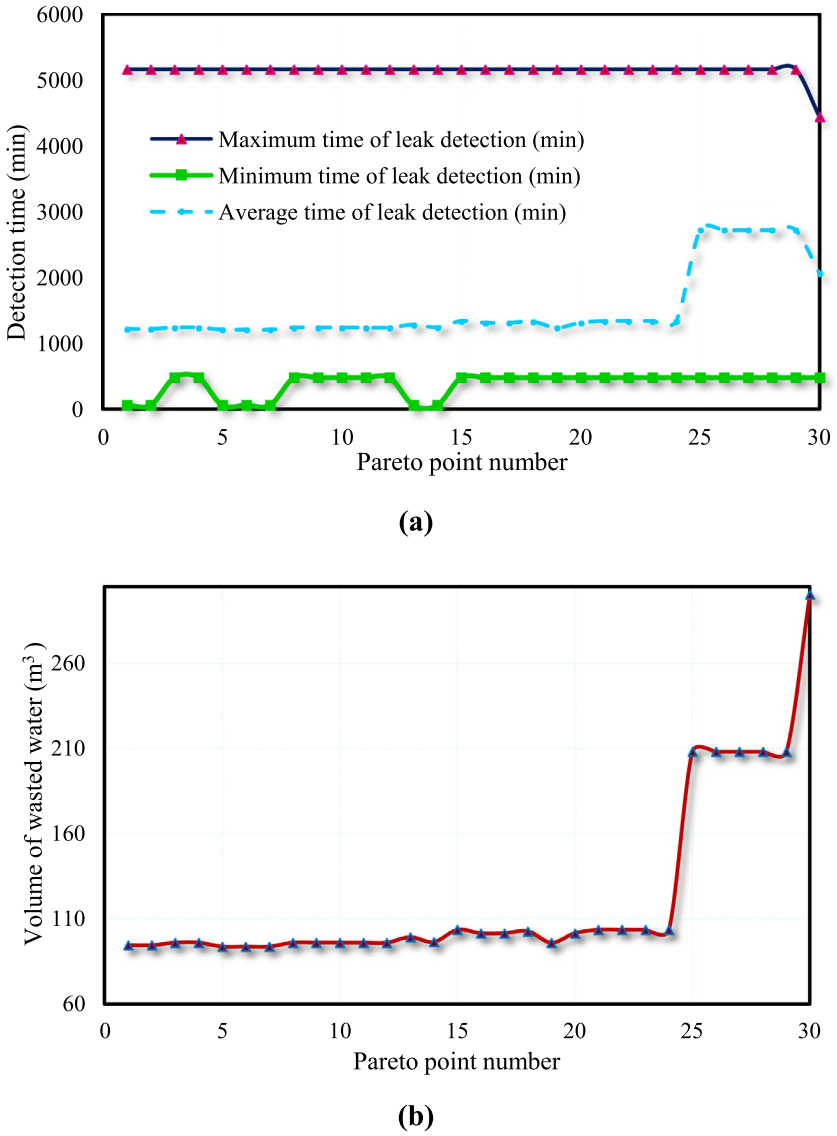

Fig. 6. (a) Average, minimum and maximum time of leak detection corresponding to the Pareto solutions and (b) the lost volume of water due to leakage.

range with a *Wd* of 94.95 m^3. Similar to *Td*, the volume of leaked water for R2 and R3 are far from this range, as *Wd* for R2 and R3 are equal to 121.75 m^3 and 101.7 m^3, respectively. This shows that there are at least a few layouts of Pareto points obtained from the herein proposed framework that outperforms the layouts obtained from other methods (here, R1, R2, and R3).

To deepen the understanding of the trade-off between various solutions, Fig. 6 provides detailed information associated with Pareto optimal solutions. Average, maximum, and minimum time of leak detection corresponding to each optimum solution is shown in Fig. 6a. It is clear that in a majority of the solutions, average time to leakage detection is about 20 h. Also, Fig. 6b illustrates information about the volume of water that was lost in each optimum solution. A higher number of pressure sensors and a higher value of information expectedly resulted in lower water loss. Placing 10 pressure sensors (e.g., Pareto point #1) in WDN provides more valuable information, in which about 94.66 m^3 of water may be lost to leakage, and less time would be required to detect leakage. When placing only two pressure sensors (e.g., Pareto point #25), water loss would be about 208 m^3 and the time of detection would be higher. It is clear that time of detection and volume of lost water are directly and positively correlated. In Pareto point #25, both detection time and volume of wasted water spiked, meaning that decreasing number of sensors from 3 (Pareto point #24) to 2 (Pareto point #25) has a significant effect on increasing the time of leak detection as well as the volume of wasted water.

As the final step, the ELECTRE decision-making model was developed and applied to select the best compromise solution among those rendered by NSGA-II. In the decision-making process, criteria may have different weights (different impor-

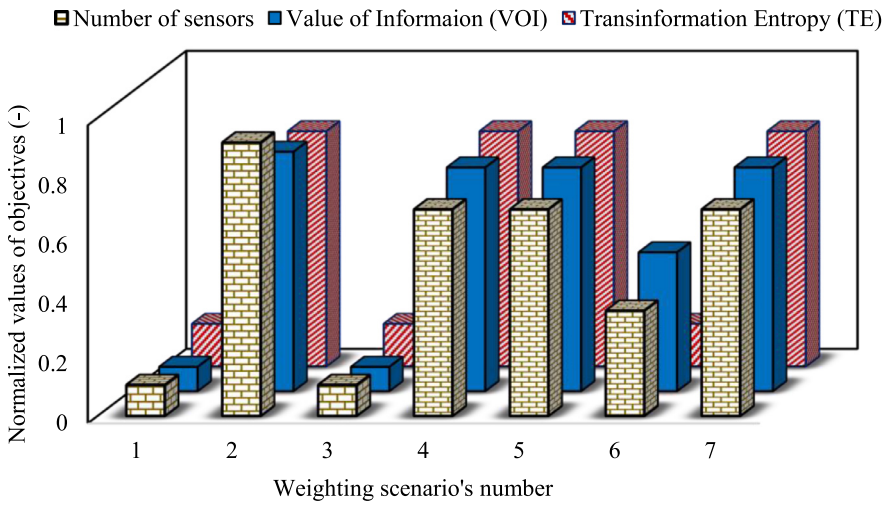

Fig. 7. Sensitivity analysis based on the normalized values of three main criteria in seven weighting scenarios.

Table 5
Weighting scenarios for the three optimization criteria.

Weighting scenarios	Criterion 1 (No. of sensors)	Criterion 2 (VOI)	Criterion 3 (TE)
1	0.7	0.15	0.15
2	0.15	0.7	0.15
3	0.15	0.15	0.7
4	0.4	0.4	0.2
5	0.2	0.4	0.4
6	0.4	0.2	0.4
7	0.33	0.33	0.33

Table 6
Result of the ELECTRE decision-making model for seven weighting scenarios.

Weighting scenario	Selected solution	ELECTRE score	Criteria		
			No. of sensors	VOI (dimensionless)	TE (dimensionless)
1	30	24	1	173	0
2	22	20	4	288	1
3	30	24	1	173	0
4	24	22	3	279	1
5	24	22	3	279	1
6	25	23	2	240	0
7	24	22	3	279	1

tance). As shown in Table 5, seven different weighting scenarios were assigned to the three mentioned criteria to perform a sensitivity analysis.

Fig. 7 shows the results of sensitivity analysis of the three decision criteria (objectives) in seven weighting scenarios of this study. All criteria are sensitive to the weighting scenarios and are changed by each scenario significantly. Using Eqs. (12)–(19), the best solution, according to each weighting scenario were determined. Table 6 enlists the results of the decision-making process.

If the objective function 1 (number of sensors) receives a higher weight (more importance) and the others receive similar weights, solution #30 with one sensor would be chosen, while in this condition the VOI value is low, and rationally, the TE value is zero. If the second objective, i.e., VOI, receives a higher weight, the best solution would be selected as Pareto point #22 with four sensors. If the third objective, i.e. TE, receives a higher weight, the number of required sensors would be one. Fig. 8 shows the placement of sensors in the selected Pareto optimal solutions in all weighting scenarios. Moreover, the average detection time corresponding to solutions #22, 24, 25 and 30 are about 22, 22, 45 and 34 h, respectively. These results show that placing more than three sensors helps precise detection of the leak event in a timely manner. Raei et al. [32] reported placing 20 sensors can detect the leakage in 19 h, while in this study, with the aid of VOI and TE, only three sensors can provide leak detection in 22 h.

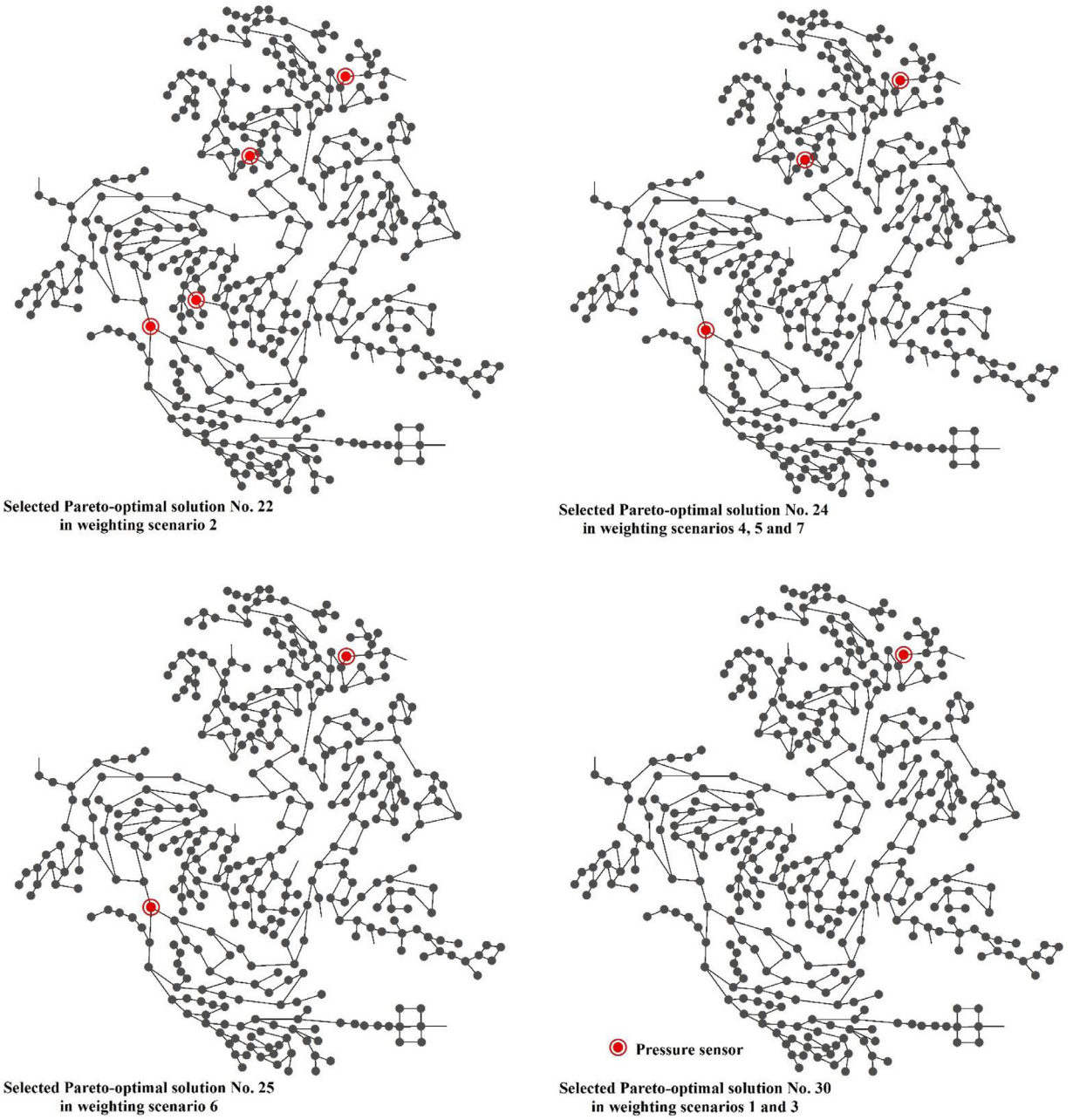

Fig. 8. Sensor placement layout in four selected optimal solutions by the ELECTRE decision-making model.

5. Summary and conclusion

In this study, a novel simulation-optimization approach that benefits from information theory is proposed to detect leakage events in Water Distribution Networks (WDNs). In the first step, the WDN was simulated using the EPANET numerical model forced by diurnal water demands, and the pressure values of all nodes were determined in two conditions: with and without leakage scenarios. In the second step, the NSGA-II optimization model was used – given the information provided in the first step about pressure differences in various nodes induced by leakage – to determine the optimal sensor placement layouts with three objectives: minimizing the number of sensors, minimizing the Transinformation Entropy (TE), and maximizing the Value of Information (VOI). VOI provides a measure of the value of each sensor in detecting leakage, and

TE renders a measure of the uniqueness of information provided by different sensors. Hence, VOI informs best detecting sensors and TE maximizes the spatial coverage of sensor layout. This approach resolves a significant shortcoming of the previously proposed leak detection frameworks, namely their high computational costs. Applying a hybrid VOI-TE approach minimizes the computational costs and provides superior solutions to the methods proposed in the literature.

Previous studies curbed the computational burden of sensor placement methods by confining the decision space to a limited set of potential nodes [32]. This approach is subjective and disregards some nodes that can potentially provide acceptable results. VOI was employed in this study to explore the entire decision space and investigate the best layout of sensors in WDN. The layout determined by VOI, however, may include redundant information that imposes additional installation and maintenance cost. Thus, the TE method was coupled with VOI to decrease the mutual information among pressure sensors and maximize spatial coverage of sensors.

In this framework, the NSGA-II multi-objective model was implemented, which provided 30 Pareto optimal solutions. The obtained solutions from NSGA-II contain a number of sensors between 1 to 10. Since the selection of the best pressure sensor layout depends on utility providers' priorities, the ELECTRE multi-criteria decision-making model was employed to select the best compromise solution. Seven weighting scenarios were considered to determine the effect of different priorities on the final layout. Finally, the best solution in each weighting scenario was determined, which pointed to the importance of weighting scenarios on the layout configuration.

In conclusion, coupling VOI and TE resulted in a lower number of pressure sensors and a higher probability of leak detection with lesser computational time. Authors' suggestions for future studies include: (i) analyzing uncertainty in pressure sensors detection threshold, water demand and/or water discharge of WDN using fuzzy set theory [37,38] and interval programming [26,43], (ii) applying the herein proposed methodology considering both pressure sensors and flow meters, (iii) using clustering methods in order to improve detection precision in each pressure zone, (iv) developing a spatial variogram alongside and/or instead of TE to determine the minimum redundant information, and (v) using a conflict resolution model to resolve conflict between differnet competing stakeholders [42,44].

Declaration of Competing Interest

The authors declare that they have no competing interests and no conflicting interests.

CRediT authorship contribution statement

Mohammad Sadegh Khorshidi: Formal analysis, Writing - review & editing. **Mohammad Reza Nikoo:** Conceptualization, Writing - review & editing. **Narges Taravatrooy:** Writing - original draft, Writing - review & editing. **Mojtaba Sadegh:** Writing - review & editing. **Malik Al-Wardy:** Writing - review & editing. **Ghazi Ali Al-Rawas:** Writing - review & editing.

References

[1] L. Alfonso, R. Price, Coupling hydrodynamic models and value of information for designing stage monitoring networks, Water Resour. Res. 48 (8) (2012) 1–13.
[2] L. Alfonso, M.M. Mukolwe, G. Di Baldassarre, Probabilistic Flood Maps to support decision-making: mapping the value of information, Water Resour. Res. 52 (2) (2016) 1026–1043.
[3] Z. Alizadeh, J. Yazdi, A. Moridi, Development of an entropy method for groundwater quality monitoring network design, Environ. Process. 5 (4) (2018) 769–788.
[4] O. Ameri Sianaki, Intelligent decision support system for energy management in demand response programs and residential and industrial sectors of the smart grid Ph.D. Thesis, Curtin University, 2015.
[5] S. Ashraf, A. Aghakouchak, A. Nazemi, A. Mirchi, M. Sadegh, H.R. Moftakhari, E. Hassanzadeh, C.Y. Miao, K. Madani, M.M. Baygi, H. Anjileli, D.R. Arab, H. Norouzi, O. Mazdiyasni, Compounding effects of human activities and climatic changes on surface water availability in Iran, Clim. Change 152 (3-4) (2019) 379–391.
[6] AVNET, (2019). www.avnet.com/wps/portal/abacus/solutions/technologies/sensors/pressure-sensors/media-types/water/, last retrieved on 18 October, 2019.
[7] M. Beccali, M. Cellura, M. Mistretta, Decision-making in energy planning application of the electre method at regional level for the diffusion of renewable energy technology, Renew. Energy 28 (13) (2003) 2063–2087.
[8] A. Bennett, B. Nijssen, G. Ou, M. Clark, G. Nearing, Quantifying process connectivity with transfer entropy in hydrologic models, Water Resour. Res. 55 (6) (2019) 4613–4629.
[9] A. Boroumand, T. Rajaee, F. Masoumi, Semivariance analysis and transinformation entropy for optimal redesigning of nutrients monitoring network in San Francisco bay, Marine Pollut. Bull. 129 (2) (2018) 689–694.
[10] C. Capponi, M. Ferrante, A.C. Zecchin, J. Gong, Leak detection in a branched system by inverse transient analysis with the admittance matrix method, Water Resour. Manag. 31 (13) (2017) 4075–4089.
[11] K. Deb, Multi-Objective Optimization Using Evolutionary Algorithm, John Wiley and Sons, LTD, Chichester, UK, 2000.
[12] J.A. Goulet, S. Coutu, F.C. Smoth, Model falsification diagnosis and sensor placement for leak detection in pressurized pipe network, Adv. Eng. Inf. 27 (2013) 261–269.
[13] C.J. Grayson, Decisions Under Uncertainty: Drilling Decisions by Oil and Gas Operators, Ayer. (Publisher: Harvard Business School, 1960.
[14] J. Hirshleifer, J.G. Riley, The analytics of uncertainty and the information an expository survey, J. Econ. Lit. 17 (4) (1979) 1375–1421.
[15] M. Hosseini, R. Kerachian, A data fusion-based methodology for optimal redesign of groundwater monitoring networks, J. Hydrol. 552 (1) (2017) 267–282.
[16] M.S. Khorshidi, M.R. Nikoo, M. Sadegh, Optimal and objective placement of sensors in water distribution systems using information theory, Water Res. 143 (2018) 218–228.
[17] M.S. Khorshidi, M.R Nikoo, E. Ebrahimi, M. Sadegh, A robust decision support leader-follower framework for design of contamination warning system in water distribution network", J. Clean. Prod. 214 (2019) 666–673.

[18] M.S. Khorshidi, M.R Nikoo, M. Sadegh, B. Nematollahi, A multi-objective risk-based game theoretic approach to reservoir operation policy in potential future drought condition, Water Resour. Manag. 33 (6) (2019) 1999–2014.
[19] N. Mahjouri, R. Kerachian, Revising river water quality monitoring networks using discrete entropy theory: the Jajrood River experience, Environ. Monit. Assess. 175 (2011) 291–302.
[20] F Masoumi, R Kerachian, Optimal redesign of groundwater quality monitoring networks: a case study, Environ. Monit. Assess. 161 (1-4) (2010) 247–257.
[21] N. Maymandi, R. Kerachian, M.R. Nikoo, Optimal spatio-temporal design of water quality monitoring networks for reservoirs: application of the concept of value of information, J. Hydrol. 558 (2018) 328–340.
[22] M. Memarzadeh, N. Mahjouri, R. Kerachian, Evaluating sampling locations in river water quality monitoring networks: application of dynamic factor analysis and discrete entropy theory, Environ. Earth. Sci. 70 (6) (2013) 2577–2585.
[23] Y. Mogheir, J.L.M.P. de Lima, V.P. Singh, Characterizing the spatial variability of groundwater quality using the entropy theory: I. Synthetic data, J. Hydrol. Process. 18 (2004) 2165–2179.
[24] Y. Mogheir, J.L.M.P. de Lima, V.P. Singh, Characterizing the spatial variability of groundwater quality using the entropy theory: II. Case study from Gaza Strip, J. Hydrol. Process. 18 (2004) 2579–2590.
[25] M.R. Naeini, T. Yang, M. Sadegh, A. Aghakouchak, K.L. Hsu, S. Sorooshian, Q. Duan, X. Lei, Shuffled complex-self adaptive hybrid evolution (SC-SAHEL) optimization framework, Environ. Model. Softw. 104 (2018) 215–235.
[26] M.R. Nikoo, A. Karimi, R. Kerachian, Optimal long-term operation of reservoir-river systems under hydrologic uncertainties: application of interval programming, Water Resour. Manag. 27 (11) (2013) 3865–3883.
[27] M.R. Nikoo, N. Khorramshokouh, S. Monghasemi, Optimal design of detention rockfill dams using a simulation-based optimization approach with mixed sediment in the flow, Water Resour. Manag. 29 (15) (2015) 5469–5488.
[28] R. Pérez, V. Puig, J. Pascual, A. Peralta, E. Landeros, L.I. Jordanas, Pressure sensor distribution for leak detection in Barcelona water distribution network, Water Sci. Technol. Water Supply 9 (6) (2009) 715–721.
[29] S. Pourshahabi, M.R. Nikoo, E. Raei, J.F. Adamowski, An entropy-based approach to fuzzy multi-objective optimization of reservoir water quality monitoring network considering uncertainties, Water Resour. Manag. 32 (13) (2018) 4425–4443.
[30] S. Pourshahabi, N. Talebbeydokhti, G. Rakhshandehroo, M.R. Nikoo, Spatio-temporal multi-criteria optimization of reservoir water quality monitoring network using value of information and transinformation entropy, Water Resour. Manag. 32 (10) (2018) 3489–3504.
[31] E. Raei, M.R. Nikoo, S. Pourshahabi, M. Sadegh, Optimal joint deployment of flow and pressure sensors for leak identification in water distribution networks, Urban Water J. 15 (9) (2019) 837–846.
[32] E. Raei, M.E. Shafiee, M.R. Nikoo, E. Berglund, Placing an ensemble of pressure sensors for leak detection in water distribution networks under measurement uncertainty, J. Hydroinformat. 21 (2) (2018) 223–239.
[33] E. Ridolfi, M. Rianna, G. Trani, L. Alfonso, G. Di Baldassarre, F. Napolitano, F. Russo, A new methodology to define homogeneous region through an entropy based clustering method, Adv. Water Resour. 96 (2016) 237–250.
[34] M.J. Roberts, D. Schimmelpfennig, M.J. Livingston, E. Ashley, Estimating the value of an early-warning system, Rev. Agric. Econ. 31 (2) (2009) 303–329.
[35] L.A. Rossman, Epanet 2 Users Manual, Us Environmental Protection Agency. *Water Supply and Water Resources Division*, National Risk Management Research Laboratory, Cincinnati, OH, 2000, p. 45268.
[36] B. Roy, The outranking approach and the foundations of ELECTRE methods, in: Readings in Multiple Criteria Decision Aid, Springer, 1990, pp. 155–183.
[37] M. Sadegh, R. Kerachian, Water resources allocation using solution concepts of fuzzy cooperative games: fuzzy least core and fuzzy weak least core, Water Resour. Manag. 25 (10) (2011) 2543–2573.
[38] M. Sadegh, N. Mahjouri, R. Kerachian, Optimal inter-basin water allocation using crisp and fuzzy Shapley games, Water Resour. Manag. 24 (10) (2010) 2291–2310.
[39] M.E. Shafiee, A. Berglund, E.Z. Berglund, E. Downey Brill Jr., G. Mahinthakumar, Parallel evolutionary algorithm for designing water distribution networks to minimize background leakage, J. Water Resour. Plann. Manag. 142 (5) (2016) C4015007.
[40] C.E. Shannon, A mathematical theory of communication, II and I, Bell Syst. Tech. J. 27 (1948) 379–423.
[41] V.P. Singh, The use of entropy in hydrology and water resources, Hydrol. Process. 11 (1997) 587–626.
[42] M.R. Alizadeh, M.R. Nikoo, G.R. Rakhshandehroo, Developing a multi-objective conflict-resolution model for optimal groundwater management based on fallback bargaining models and social choice rules: a case study, Water Resources Management 31 (5) (2017) 1457–1472, doi:10.1007/s11269-017-1588-7.
[43] M.R. Nikoo, P.H.B. Beiglou, N. Mahjouri, Optimizing Multiple-Pollutant Waste Load Allocation in Rivers: An Interval Parameter Game Theoretic Model, Water Resour Manage 30 (2016) 4201–4220, doi:10.1007/s11269-016-1415-6.
[44] S.M. Estalaki, R. Kerachian, M.R. Nikoo, Developing water quality management policies for the Chitgar urban lake: application of fuzzy social choice and evidential reasoning methods, Environ Earth Sci 75 (2016) 404, doi:10.1007/s12665-015-5065-4.